Original Research Paper

IJES *Iranian Journal of Earth Sciences*
Vol. 14, No. 2, 2022, 150-164.
DOI: 10.30495/ijes.2021.685384

Integration of geological and geophysical studies in order to mineral exploration at the Zaveh mineralization area, NE Iran

Bahareh Borozinyat[1], Azadeh Malekzadeh Shafaroudi[*2], Mohammad Reza Haidarian Shahri[1]

1. *Department of Geology, Faculty of Science, Ferdowsi University of Mashhad, Mashhad, Iran*
2. *Department of Geology and Research Center for Ore Deposit of Eastern Iran, Faculty of Science, Ferdowsi University of Mashhad, Mashhad, Iran*

Received 6 November 2020; accepted 9 August 2021

Abstract

The copper deposit of Zaveh lies in the SE of the city of Torbat-e-Heydarieh and in middle of the Khaf-Kashmar-Bardaskan Magmatic Belt (KKBMB) in the Khorasan-e-Razavi Province. The lithology of the area consist of Jurassic and Cretaceous sedimentary rocks and Eocene volcanic units. Ore-formation is controlled by fault activity, representing vein-veinlet style E-W trending, formed within a conglomerate rich in quartz. Primary minerals are chalcopyrite, pyrite and arsenopyrite and secondary minerals contain malachite, azurite chalcocite, bornite, covellite, Cu sulphates, wad (Mn hydroxide), haematite, goethite, jarosite, limonite and (to a lesser extent) chrysocolla. The predominant alteration is silification which is associated with vein ore-formation. The volcanic units host propylitic, sericite, carbonate and silicification alterations. The ore-formation itself represents anomalies of Cu (2.1 % max), As (>1%), Sb (~105 gr/T), Pb (4371 gr/T) and Zn (1.1% max). Induced polarization and electrical resistivity (IP/RS) surveys unveil that the most chargeability anomaly corresponds to center of ore-forming vein and fault zone.

The chargeability anomaly extends and amplifies with depth. The most amount of specific electrical resistance has been observed in the quartz-rich conglomerate. Interpretation of IP/RS data reveals that the chargeable source is extending in deeper beds (presumably sulphid ore-formation) which needs to be verified by boring operation. Geophysical surveys are significantly commensurate with field observations, ore-forming and geochemical data. Utilization Geophysical methods in different style of ore-deposits and interpretation of obtained information by means of geological, ore-forming and geochemistry data is considered to be a big step towards subterranean exploration and deposits modeling.

Keywords: *Ore-formation, alteration, geochemistry, geophysics, Zaveh.*

1. Introduction

The study area is located in the NE of Iran in the Khorasan Razavi Province, ~174 km south of the city of Mashhad (Fig 1a). The coordinates of the Zaveh area are E 59°25′26″and N 35°12′6″-35°13′21″. Structurally, the area sits in the Sabzevar Zone and in the middle part of the Khaf-Kashmar-Bardaskan Magmatic Belt (KKBMB). Karimpour et al. (2006) have known the volcanic-intrusive belt of KKBMB as an overarching metallogeny expanse for Cu-Au deposits along with iron oxide (IOCG). This magmatic belt demonstrates a high potential for exploration of Fe, Cu, Au, Ag as well as non-metallic mineral deposits. The magmatic belt has expanded at the south of the Sabzevar-Torbat-e-Heydarieh Ophiolites during the Cretaceous-Plio-Quaternary reaching up to 350 km in length and 15-90 km in width (Almasi 2016 and Mazhari et al. 2016). The KKBMB has been formed by Tertiary acidic to medium and mafic rocks. These rocks show a dacitic-andesitic combination and they have been intruded by granitoid masses of a combination of granite, granodiorite and diorite (Karimpour and Malekzadeh 2006; Mollai et al. 2022).

----

*Corresponding author.

E-mail address (es): shafaroudi@um.ac.ir

The tectonic setting and magmatic variety of rocks have made the belt to host a lot of mineral reserves such as porphyry Cu-Au of the Tanurjeh area, skarn magnetite of Sangan, IOCG of Kuhzar in Torbat-e-Heydarieh and Au-bearing masses in the north of Tanurjeh (Karimpour et al. 2006). Figure 1 shows the KKBMB and geographic location of Zaveh.

The exploration report of Zaveh Cu deposit has been prepared by a mining firm named Moein Sabzehkaran. The report incorporates geological, geochemical and ore-forming information. These data are the result of study of geology and topography maps, thin sections, geochemical analyses, borehole and trenches (Roshanravan 2014). The geochemical analyses were not used in the present study due to the lack of geographical coordinate. Additionally, the study of core samples was dismissed due to their being in disorder. Based on studies conducted by Borouziniyat et al. (2019) Zaveh deposit is a Cu, As, Pb and Zn hydrothermal vein type. The geophysical studies have been conducted by way of the induced polarization and electrical resistivity (IP/RS) method. Four pseudo-vertical profiles across the ore-forming vein are designed by the Moein Sabzehkaran Co. (Kazem Alilo 2014). The IP/RS method has already been applied in the determination of location, expansion and depth of sulphide ore-formation within a different deposits such as the Garmaab Cu Deposit in south Khorasan province (Aadelpour et al. 2016), the Mahoor Deposit in the NW of Dehsalm (Ghaffari et al. 2013; Gorabjeiri Puor and Mobasheri 2014), Gazoo exploration prospect (Mahdavi et al. 2013, Sarem et al. 2015), epithermal Au deposits in Australia (Hoschke and Sexton 2005), porphyry deposit of Pebble in Alaska State (Shah et al. 2009), deep massive sulphide explorations in Sweden (Mahdavi et al. 2015; Tavakoli et al. 2016; Yazdi et al. 2022), IOCG deposits and porphyry Cu in Chile (Aguilef et al. 2017) and a Cu deposit in Mongolia (Gharib-Gorgani et al. 2017; Zhdanov et al. 2018). In this paper, we present the results of interpretation of geological, mineralization and geochemical information with an emphasis on the geophysical data in the Zaveh area in order to investigate the depth and expansion of the ore-formation process.

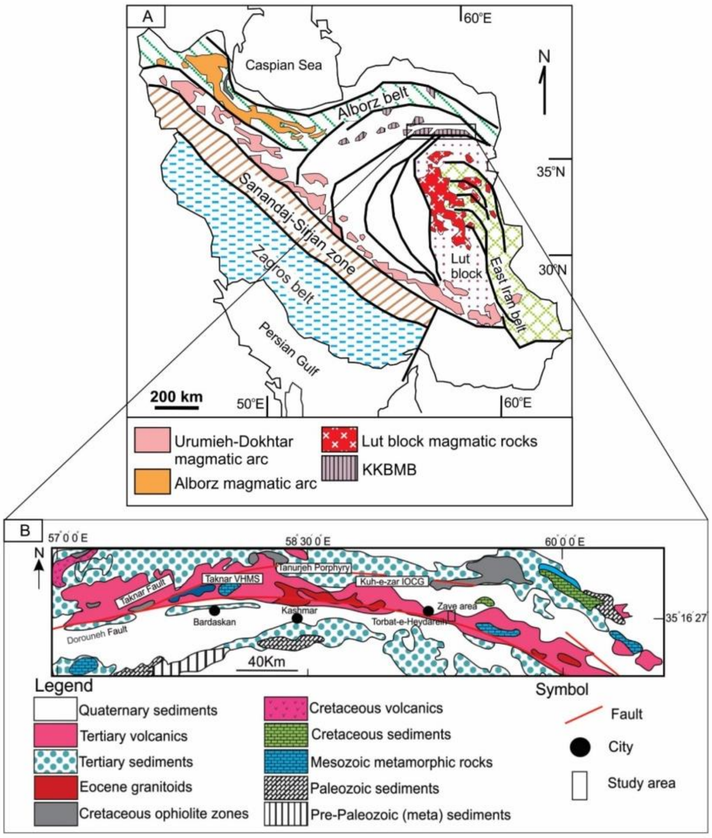

Fig 1. A) The location of KKBMB in Iran. B) The location of the Zaveh area along with other remarkable ore-forming locations within the belt (Courtesy: Darooneh 1:100000 map (Ghaemi and Mossavi Harami 2006). Bardaskan (Shahrabi et al. 2006), Kashmar (Taheri and Shmaanian 1998), Feyz Aabad (Behrouzi 1987), Torbat-e-Heydarieh (Kholghi Khasraghi 1996), Dolat Abad (Kholghi Khasraghi 1990) and Karizno (Eftekharnejad et al. (2004).

2. Methodology

Detailed field mapping was carried out to produce geological, mineralization, alteration maps within an area of about 1 km^2. In order to implement the petrography, alteration and ore-formation studies, 170 rock samples were taken. Thirty of these samples were related to mineralization studies and seventy thin-sections were studied for petrography and alteration. The geology-mineralization-alteration maps of 1:2000 were prepared in the Arc GIS Suite. Ten rock chip samples were collected from the trenches for geochemical investigations. After grinding and softening (a preparation method which is conducted through nitrification), the ten samples were analyzed through the ICP-OES (aqua regia, twenty-six elements) and Fire Assay method and two samples were selected for XRD analysis in order to identify the minerals forming alteration and ore-forming zones in the ZarAazma Laboratory. The maps of elements' shifts along the ore-forming vein were drawn in the ArcGIS Suite. Applying the ArcGIS and CorelDRAW softwares, geology profiles were prepared for IP/RS profiles and ultimately, the IP/RS data were analyzed and interpreted based on geological, alteration, mineralization and geochemical data.

3. Geological background

The study area lies in the east part of the 1:100000 geology map of Torbat-e-Heydarieh (Kholghi Khasraghi

1996). Tectonically, the area is significantly active and has an assortment of faults. The Dorooneh Fault is one of the most important fault which located in the south of Zaveh. The area is categorized into 2 groups of rocks: Eocene volcanic rocks and Jurassic-Cretaceous sedimentary rocks (Fig 2). Part of sedimentary rocks are attributed to the Shemshak Formation that have out crop in the south. The formation consists greyish-green sandstones and olive shales (Fig 2). The most important rock unit in the area is known as the quartz-rich conglomerate due to hosting the ore-forming process. The out crop of this unit is in the south of area and contiguous to the Shemshak formation (Fm) that have E-W trending and 1 km length (Fig 2). Fe oxide has imparted a red color to the rocks, while the cream and light brown-cream colors are due to silica and carbonate. The conglomerate possesses a lot of monocrystalline, polycrystalline, metamorphic and silicification alteration of the quartzes. The red sandstone crops out in an intercalation fashion within the conglomerate (the red sandstone was also pinpointed in the center of the study area). Around 95% of the material forming the sandstone are quartz grains, although feldspar, glauconite and sedimentary debris e.g. chert are the another material-forming materials. The limestone unit in the area has restricted expansion, due to the tectonism occurring as exiguous individual masses at the border of pyroxene trachy-andesite with quartz-rich conglomerate E-W trending (Fig 2). It is grey and at some parts, it is creamy. The unit consists of orbitolina-bearing

micrite lime with interlayers of calcite and dolomite of 1-2.5m thickness in between. The pyroxene trachy-andesite has expanded the most in the area (Fig 2). This unit has a porphyry and glomo-porphyry texture in a fine-to medium-grain matrix and 25-30% of phenocrysts. The phenocrysts include plagioclase, alkali-feldspar and clino-pyroxene. Pyroclastic breccias of quartz trachy-andesite have outcrop contiguous to the trachy-andesite unit (Fig 2). Bombs and blocks of 0.5-50cm diameter have formed the clasts. Plagioclase and alkali-feldspars in volcanic rocks have, generally, transformed into sericite and carbonate. And pyroxene has intensely transformed into chlorite.

A dike of pyroxene monzodiorite porphyry E-W trending and lying in the quartz-rich conglomerate has cropped out. It has 600m length and it is 2-3m thick. The predominant texture is porphyry with the crystals. And matrix has been intensely transformed by the propylitic and carbonate styles of alteration. The phenocrysts include pyroxene, plagioclase and alkali-feldespar that are present in the chloritic and carbonate matrix. This unit does not have any mineralization.

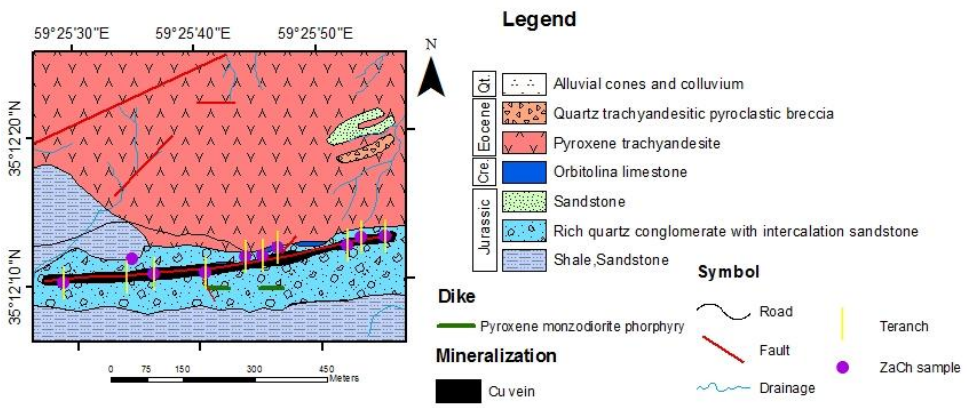

Fig 2. The geological-mineralization map of Zaveh.

4. Mineralization and alteration

The quartz-rich conglomerate hosts ore-formation in the Zaveh area (Fig 3). The mineralization has occurred as veins and veinlets E-W trending and along a fault (Fig 2). The ore-forming vein has ~ 900m length, 1.5-2m width and a northwardly dip of 60-65°. The primary ore-formation consists of arsenopyrite (25-30%), pyrite (15-20%) and chalcopyrite (10-15%) (Fig 4A-C).

The texture of pyrite and chalcopyrite is massive and disseminated while this appears as disseminated, massive and veinlet of 0.1 thickness for arsenopyrite. Arsenopyrite, chalcopyrite and pyrite themselves are mainly anhedral to subhedral measuring from a few microns up to 2mm. The secondary minerals entail malachite, azurite, chalcocite, bornite, covellite, haematite, goethite, jarosite, limonite, wad (Mn hydroxide), Cu sulphate and chrysocolla (in minor amount). Most veinlet, disseminated, secondary replacement and colloform textures have hosted the ore-formation process. The veinlet texture is the most important and copious style of mineralization in the Zaveh area.

The colloform texture has been solely spotted in malachite and in the ore-formation vein in microscopic scale. Chalcocite, bornite and covellite have been formed in replacement style due to their shift to chalcopyrite (Fig 4D).

Fig 3. Outcrops of ore-forming vein in quartz-rich conglomerate

The volume of transformations in the following minerals is 60-100% for chalcopyrite to chalcocite, 50-100% for chalcopyrite to bornite and 40-100% for chalcopyrite to covellite. Another product of mineralization has been the formation of malachite veinlets of 0.1-2mm thickness and, to a lesser extent, azurite veinlets of 0.1-0.3mm (Figs 4E and F) thickness. Goethite-quartz 0.1mm thick veinlets were spotted. Colloidal texture has been displayed in Fig 4G.

The lateral expansion of Fe-oxides around the ore-forming vein reaches up to 10m. Blue stone, jarosite and limonite are disseminated in the Gossan zone (Figs 4 H and I). Having been associated with the Zaveh vein ore-forming vein. The sort of quartz whose source has been silicification alteration is a poly-crystalline one with an obscure and disorderly rim (Fig 4J).

The secondary quartz veinlets have a mosaic texture which differs from the quartz conglomerates of coarse and distinguishable crystals. Accomodating 35% of the total volume of rock, silica is spotted as veinlets of 0.1-3mm thickness and also as disseminated in the matrix. The quartz-bearing veinlets are categorized into four types:

1. Quartz veinlets of ~1-3mm,
2. Goethite±quartz veinlets of 0.1mm thickness in which quartz volume varies between 10-45%,
3. Malachite±quartz veinlet of 0.1-2mm thickness in which quartz volume varies between 5-60%,
4. Arsenopyrite±quartz veinlet of 0.2mm thickness in which quartz volume varies between 10-30%.

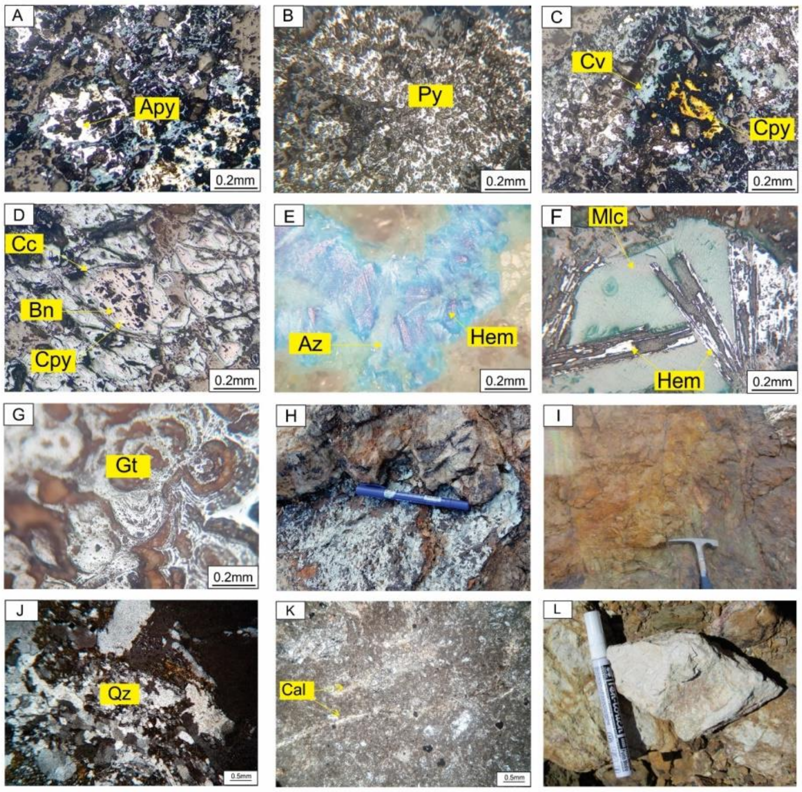

Fig 4. Mineralization in the Zaveh area, A) arsenopyrite of massive and disseminated texture in ppl, B) pyrite of massive texture in ppl, C) chalcopyrite of massive texture transforming into covellite in ppl, D) bornite and calcosite of replacement secondary texture which are results of transformation of chalcopyrite and bornite in ppl, respectively, E) association of azurite and haematite in ppl, F) association of malachite and haematite in ppl, G) goethite of cauliflower texture in ppl, H) Cu sulphate or blue stone in the wall of ore-forming vein, I) haematite and limonite in the wall of the ore-forming vein, J) silicification alteration in xpl, K) carbonate alteration, L) argillic alteration in hand specimen (arsenopyrite=Apy, pyrite=Py, calco-pyrite=Cpy, covellite =Cv, malachite= Mlc, bornite=Bn, azurite=Az, haematite=Hem, goethite=Gt, chalcocite= Cc, calcite= Cal and quartz= Qz (Whitney and Evans (2010)).

After silicification alteration, the profusion of carbonate alteration is much higher. Carbonate has formed disseminately, in the form of veins and within the quartz-rich conglomerate cement (Fig 4K).
The carbonate veinlets vary from 0.05-1mm in thickness. The profusion of carbonate sums up to 20% of total rock volume. The intensity and expansion of propylitic alteration is trifling (10%) while chlorite and epidote have been spotted in quartz-rich conglomerate cement and pore spaces. The argillic alteration was certified by field surveys and XRD analyses. This alteration has chiefly occurred in the center of the ore-forming vein while decreasing outwardly towards both sides of the vein (Fig 4L). Conducting XRD on quartz-rich samples, some trifling amount of illite was foundas the mineral in the argillic zone. Quartz, chlorite, calcite, muscovite, goethite, vesuvianite and albite were also among the other identified clay minerals (Table 1).

Table 1: Results of analysis of 2 samples from the quartz-rich conglomerate through XRD.

Sample	longitude	latitude	Major hase(s)	Minor Phase(s)	Trace Phase(s)
ZACH3	″ 59°25′ 36	″ 35°12′ 10	Quartz SiO_2	Chlorite $(Mg,Fe)_6(Si,Al)_4O_{10}(OH)_8$	-
				Muscovite- Illite $KAl_2Si_3AlO_{10}(OH)_2$	
ZACH4	″ 59°25′ 40	″ 35°12′ 10	Quartz SiO_2	Chlorite $(Mg,Fe)_6(Si,Al)_4O_{10}(OH)_8$	Vesuvianite $Ca_{19}(Al,Mg,Fe)_{11}(Si,Al)_{18}O_{69}(OH)_9$
				Muscovite- Illite $KAl_2Si_3AlO_{10}(OH)_2$	Albite $NaAlSi_3O_8$
				Calcite $CaCO_3$	
				Goethite $FeO(OH)$	

The paragenesis sequence of the Zaveh deposit is divided into hypogene and oxidized zones. The mineral-bearing fluid carrying Cu, Fe, As and Si has penetrated through the quartz-rich conglomerate by means of the faults and fractures during the hypogene stage, forming pyrite, arsenopyrite and chalcopyrite along with quartz in pore spaces between fragments and cement or within the fractures themselves. Significant volumes of arsenopyrite are signature to reduction nature of mineral-bearing fluid. Ore-forming process has surfaced in oxidant stage and has been disturbed by weathering and superficial oxidation. The process has instigated shift of primary to Cu sulphide secondary minerals e.g. chalcocite, covellite, bornite to Cu carbonate and silicate minerals e.g. malachite, azurite, chrysocolla to oxide and hydroxide minerals e.g. haematite, jarosite, limonite and goethite (Fig 5).

5. Geochemistry

Geochemical samples were taken based on the chip composite sampling method. Samples were collected from trenches, perpendicular to the strike of the vein due to the vein style of ore-formation (Fig 2). Depth of trenches vary from 2-5 meters and the distance between them is not regular.

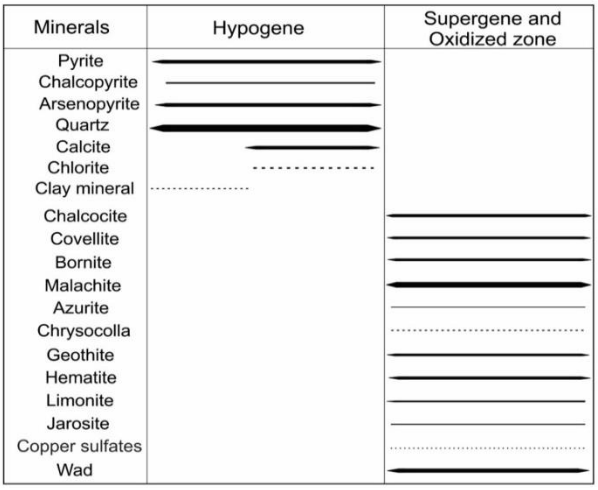

Fig 5. The paragenesis sequence of mineralization in the Zaveh area.

Obtained results from the analysis of samples are shown on Table 2. The variability amplitude of Cu is 927-21400 gr/T which is in relationship with malachite, covellite, bornite, chalcocite, azurite, chrysocolla and Chalcopyrite, with the appreciation in some sections of the ore-forming vein (Cu appreciates in volume, as well).The most significant volume of Cu lies in the center of the vein which matches with the evidence and signatures of ore-formation (Fig 6a).
Au sought in samples is not economically feasible, although the most feasible concenteration of Au is in the center of the ore-forming vein and of 56 mlg/T (Fig 6b). The amount of arsenic varies between 1820 gr/T to 1%. The most significant amount of As (>1%) has a relationship with the most abundance of arsenopyrite in the center of the vein (Fig 6c).
Amounts of Pb and Zn are 204-4370 and 815-11400 gr/T although no certain representative mineral was sought for the two elements. The foregoing numbers are likely the volumes obtained for Pb and Zn secondary minerals formed at the walls of the vein. Figs 6d and e show the shifts of the foregoing elements along the ore-forming vein. The amount of Ag is 0.86-11 gr/T which does not make sense. The amount of Fe varies between 5-8%which is due to the Gossan zone.

Table 2: Results of analysis of important elements found in geochemistry chip composite samples in the Zaveh area.

Sample	longitude	latitude	Pb	Zn	Ag	As	Cu	Sb	Fe	Au
			ppm	ppm	ppm	ppm	ppm	ppm	%	ppb
ZaCh-1	59°25′29″	35°12′10″	2720	4360	1.1	2100	1010	2.59	8.32	17
ZaCh-2	59°25′34″	35°12′10″	1270	4770	1.05	1820	1860	21.2	5.01	18
ZaCh-3	59°25′36″	35°12′10″	4370	4640	3.8	5010	1560	3.4	5.09	34
ZaCh-4	59°25′40″	35°12′10″	3790	11400	9	2740	5140	26	7.79	35
ZaCh-5	59°25′44″	35°12′11″	204	2520	3.5	7670	12100	72.2	7.34	27
ZaCh-6	59°25′45″	35°12′11″	1580	2350	2.4	3650	5450	3.41	6.14	9
ZaCh-7	59°25′46″	35°12′12″	2530	2620	11	>1%	21400	104.7	6.81	56
ZaCh-8	59°25′52″	35°12′12″	3120	815	1.5	2190	927	2.88	6.45	7
ZaCh-9	59°25′53″	35°12′12″	2180	3160	0.86	2070	2090	2.92	6.04	16
ZaCh-10	59°25′55″	35°12′13″	3210	3060	1.6	2180	1110	3.41	6.26	23

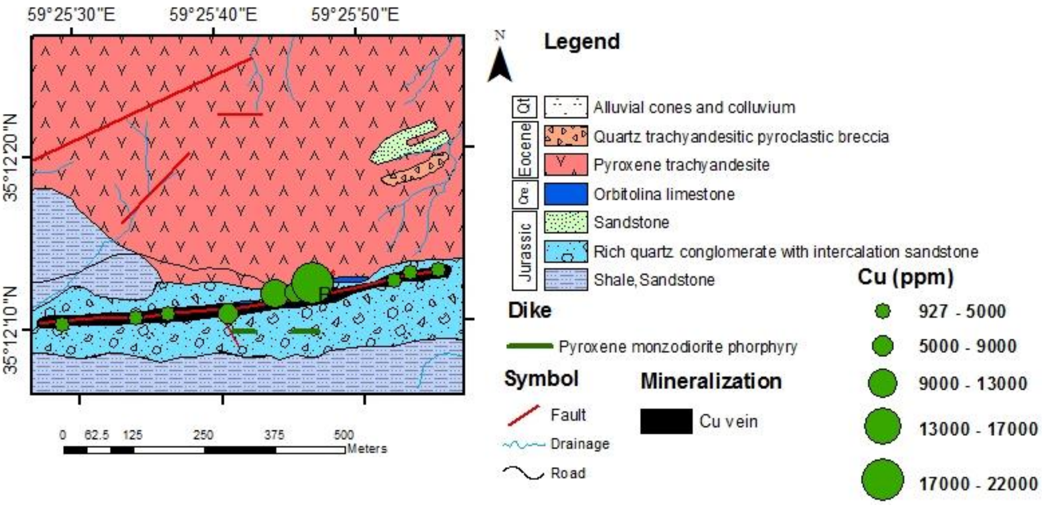

Fig 6a. The geochemical map for Cu element in the area.

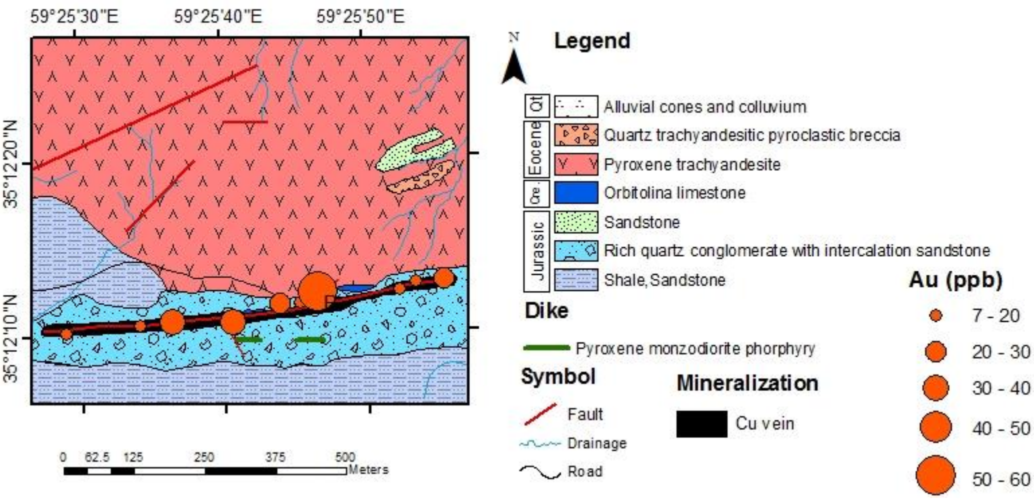

Fig 6b. The geochemical map for Au element in the area.

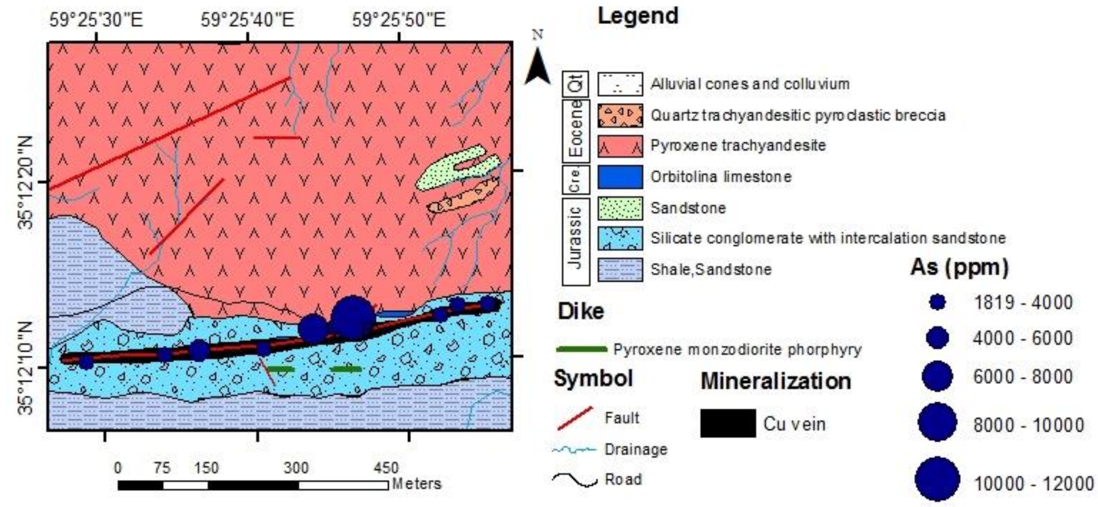

Fig 6c. The geochemical map for As element in the area.

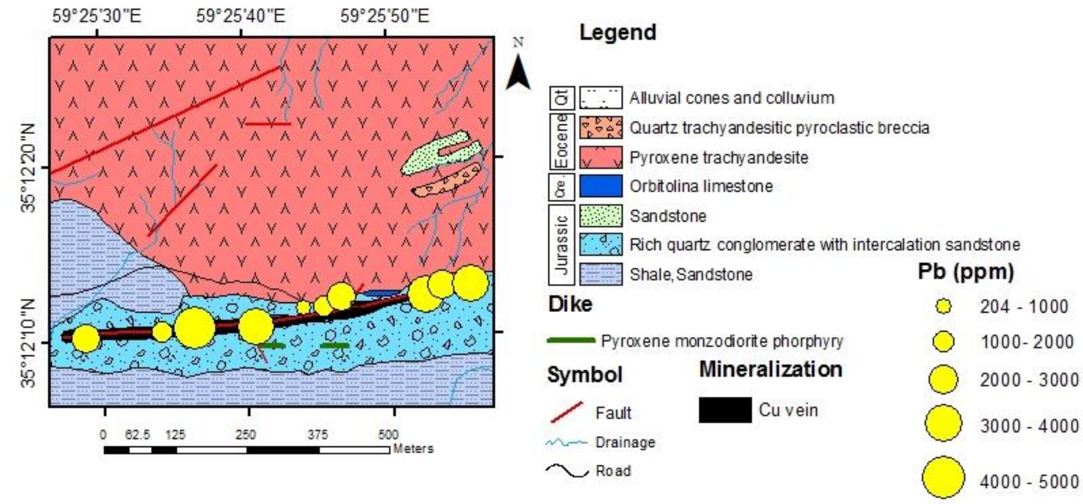

Fig 6d. The geochemical map for Pb element in the area.

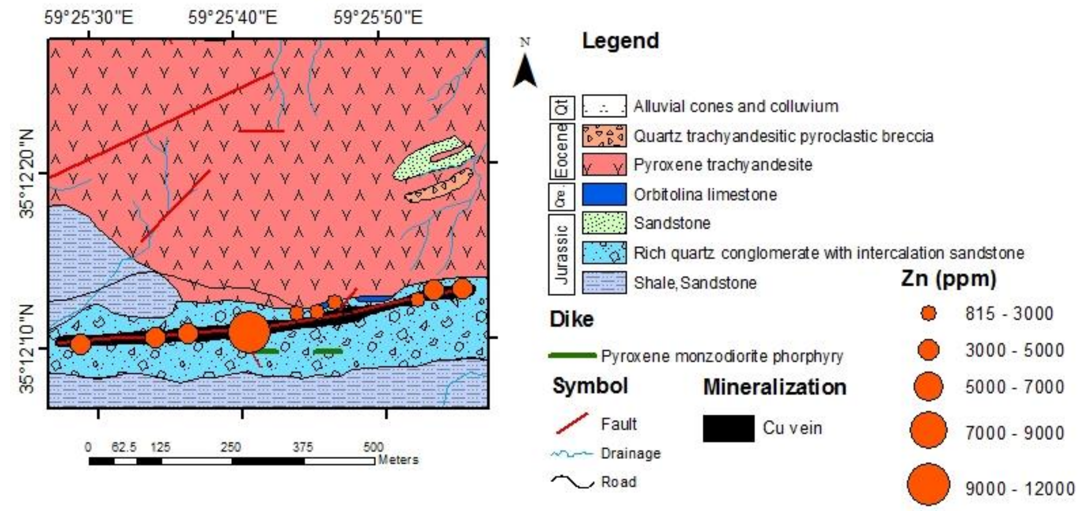

Fig 6e. The geochemical map for Zn element in the area.

One of the most noteworthy matters in geochemical surveys is to investigate the distribution pattern of elements in rock units and their dependence on each another. This would help speculate the environment and effective processes in and the variety of geological phenomena (Barnes 1997). The correlation and relationship amongst different elements in the Gossan zone have been investigated by means of Pierson Correlation Coefficient (Rollinson 1993) (Table 3).

Table 3: The numbers of coefficient correlation of each pair of elements in the Gossan zone.

	Au	Cu	As	Zn	Pb
Au	1				
Cu	0.744	1			
As	0.757	0.926	1		
Zn	0.314	-0.115	-0.208	1	
Pb	0.227	-0.322	-0.241	0.370	1

There is a positive correlation between Au-Cu and Au-As. With the minor amount of Au in the analyses, it is believed that Au would be present in the structure of arsenopyrite. More to the point, Cu and As show a high positive correlation which is interpreted as the close association of arsenopyrite with primary and secondary Cu-bearing minerals in the veins found in the Zaveh area. Pb and Zn show a poor correlation with Au. These two lack any correlation with arsenic and Cu. This suggests that the ore-formation of Pb and Zn would have occurred independent of the formation phase of Cu, Au and As, sometime during a further delayed phase, leading to a geochemical zonation in the region. Also, there is a poor correlation between Pb and Zn.

6. Geophysical studies

The geophysical studies have been conducted by the IP/RS method, using a Pole-dipole array. Four profiles which were approximately perpendicular to the ore-forming vein were designed as AA′, BB′, CC′ and DD′. AA′ and BB′ were NW-SE trending and CC′ and DD′ were NE-SW trending (Fig 7). The profiles distance was 10m and penetration depth was 85m. The length of AA′, BB′ and CC′ profiles were 220m and DD′ was 260m (Kazem Alilo 2014).

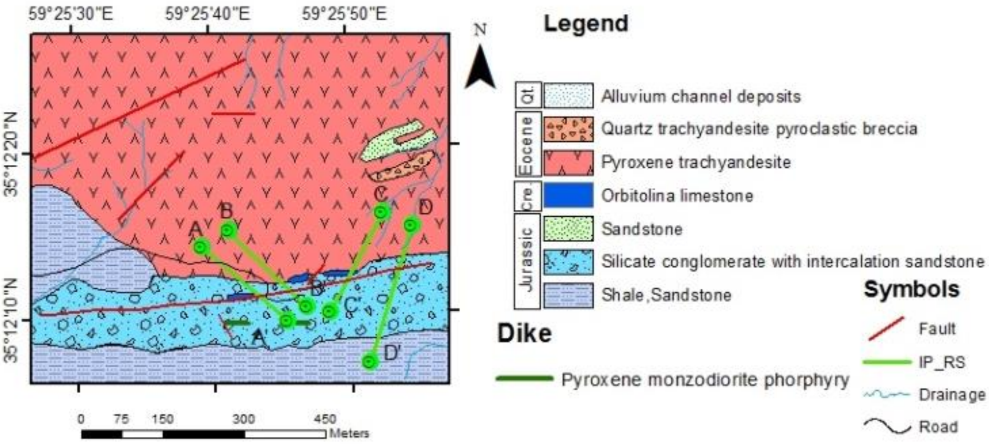

Fig 7. The location of IP/RS profiles on the geological map of Zaveh.

The chargeability anomaly of 10 mV/V at the pseudo-section of profile AA′ begins at a depth of ~20m from over the conglomeratic unit and ends at a depth of 80m. In this section, chargeability reaches up to 22 mV/V. The anomaly of chargeability expands northwardly, intensifying with depth (Fig 8B). The maximum chargeability matches with the center of the ore-forming vein, continuing towards the depth. The lowest chargeability is attributed to pyroxene trachy-andesite units. The highest level of specific electrical resistance in the pseudo-section resistivity has been spotted in the SE over the conglomerate rich in quartz (free of ore-formation). Resistivity declines northwestwardly in a sense that the specific electrical resistance declines as the resistivity enters the ore-forming zone from SE to NW (Fig 8C).

The anomaly of chargeability in the BB′ profile begins with the intensity of 10 mV/V and from the depth of 10m. The voltage reaches over 22 mV/V at depth of 60m and at the location of the ore-forming vein, continuing up to the deep depths of 80m (Fig 9B). The anomaly of chargeability of this profile expands northwardly and and it is intensified by depth. The low specific electrical resistance is consistent with the anomaly of chargeability and declines with depth (Fig. 9C).The highest specific electrical resistance has been spotted at the beginning of the profile and is attributed to the conglomerate unit rich in quartz with a declining trend in specific electrical resistance inversely related to chargeability, representing lithology response.

The anomaly of chargeability in profile CC′ of 10 mV/V intensity over the conglomeratic unit begins at a depth of <10m reaching up to 22 mV/V at 38m in the location of the ore-forming vein. The anomaly of chargeability occurs at shallower depths compared to those of AA′ and BB′, losing some of its expansion, as well (Fig 10B). It can be learned from the chargeability pseudo-section of this profile that the volume and expansion of the source has declined. Notwithstanding, the specific electrical resistance in this profile declines from SW to NE, showing the lowest specific electrical resistance at the depth of 30m in the central part (<50 ohm.meter).

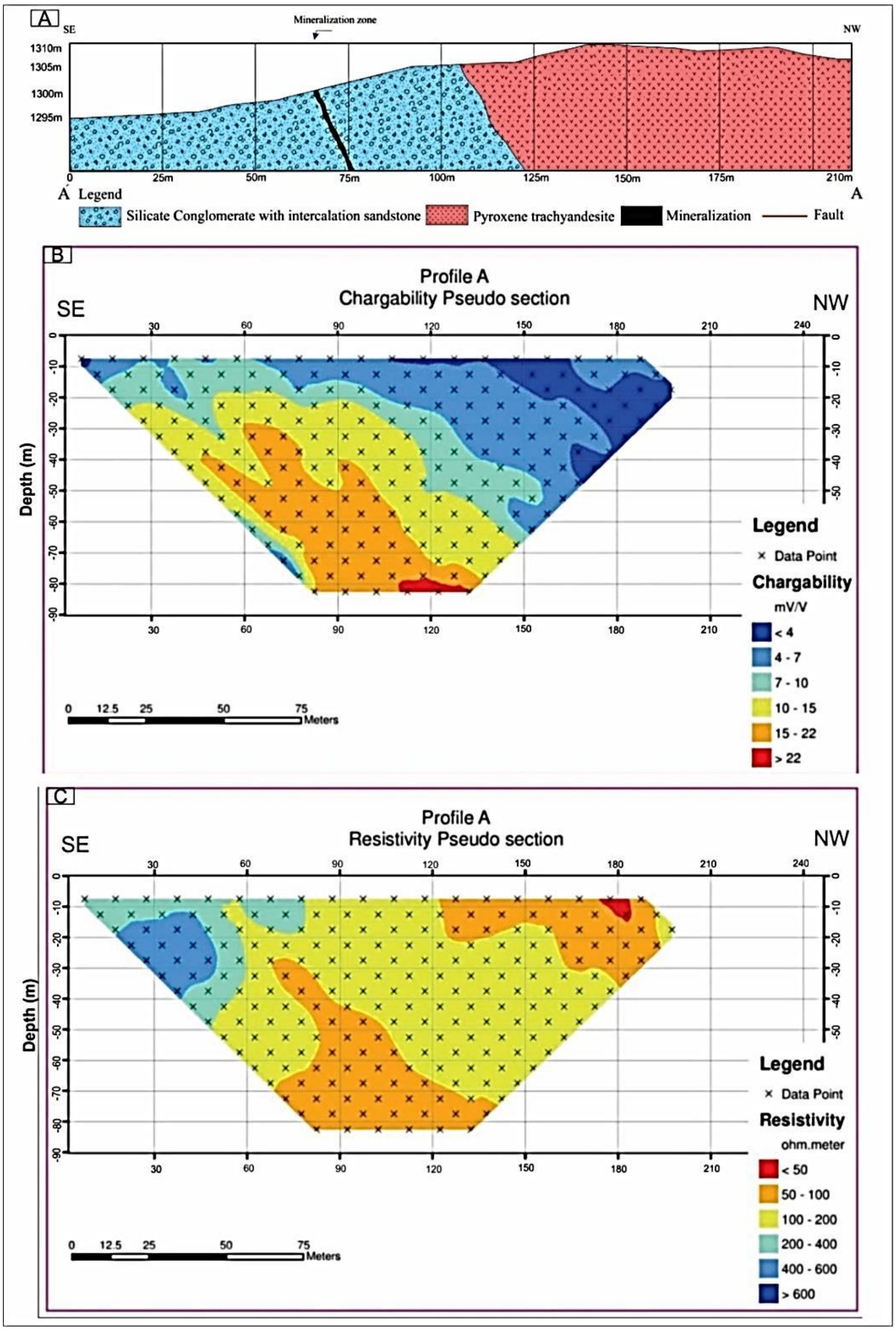

Fig 8. A) The geological profile AA′, B) the pseudo-section of chargeability profile AA′ (Kazem Alilo 2014), C) the pseudo-section of specific electrical resistance of profile AA′ (Kazem Alilo 2014).

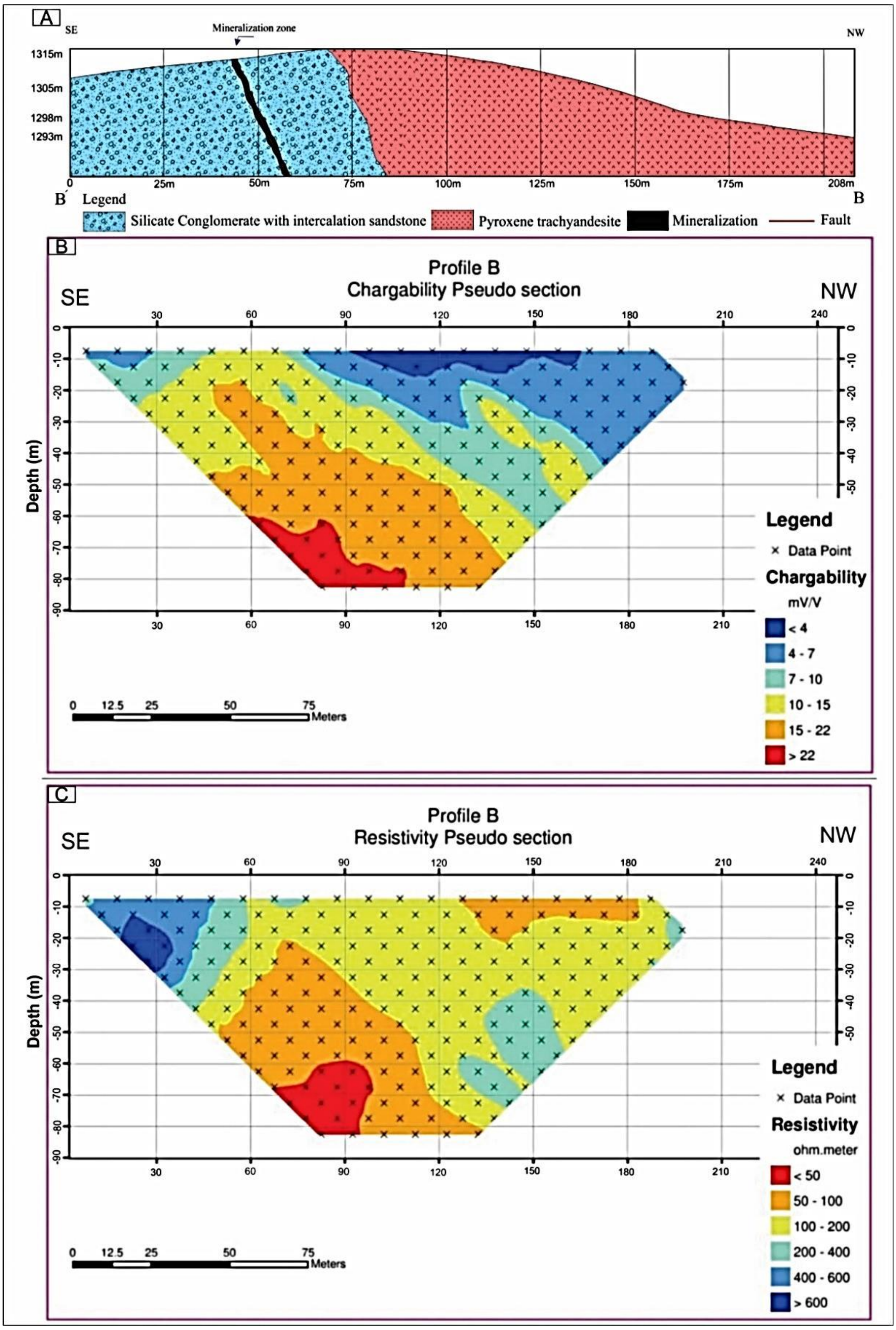

Fig 9. A) The geological profile BB', B) the pseudo-section of chargeability profile BB′(Kazem Alilo (2014)), C) the pseudo-section of specific electrical resistance of profile BB′(Kazem Alilo (2014)).

Like the previous profiles, the trend of shifts in specific electrical resistance has an inverse relationship with shifts in chargeability (Fig. 10C). A pseudo anomaly of chargeability is matched with the shale and sandstone of the Shemshak Fm. was spotted at a depth of 10m in profile DD′. Considering the fact that no ore-forming process has been sought in the shale unit, the chargeability should have been of the electrolytic sort. Therefore, it is unrealistic. Chargeability declines from SW to NE which represents a decline in electrolyte in the volcanic unit as compared to the shale unit (Fig. 11B). The specific electrical resistance pseudo-section in profile DD′ represented the lithological effects very well. The specific electrical resistance increases from shale to quartz-rich conglomerate unit while it decreases northeastwardly over the volcanic unit (Fig 11C).

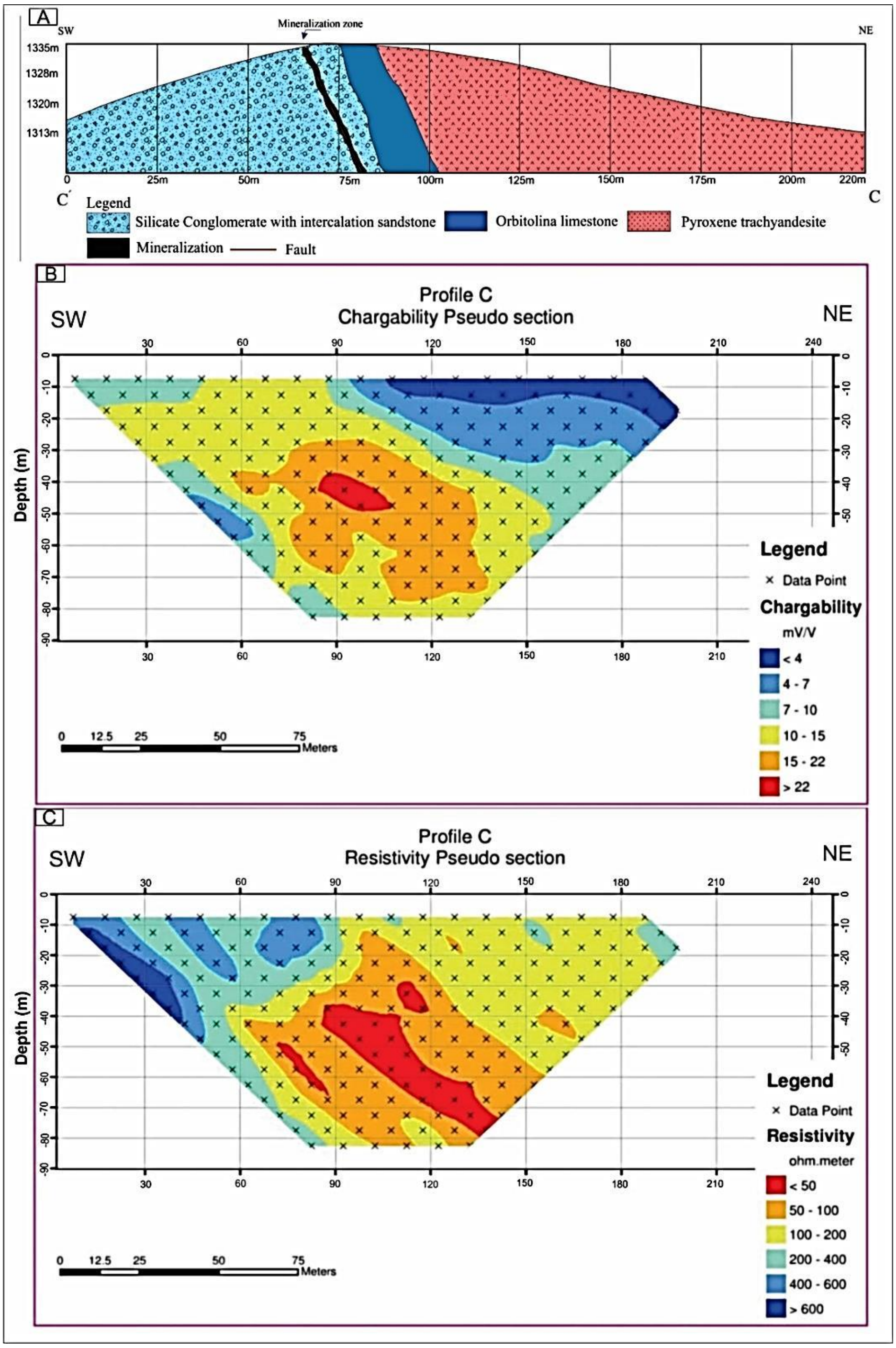

Fig 10. A) The geological profile CC′, B) the pseudo-section of chargeability profile CC′ (Kazem Alilo 2014), C) the pseudo-section of specific electrical resistance of profile CC′ (Kazem Alilo 2014).

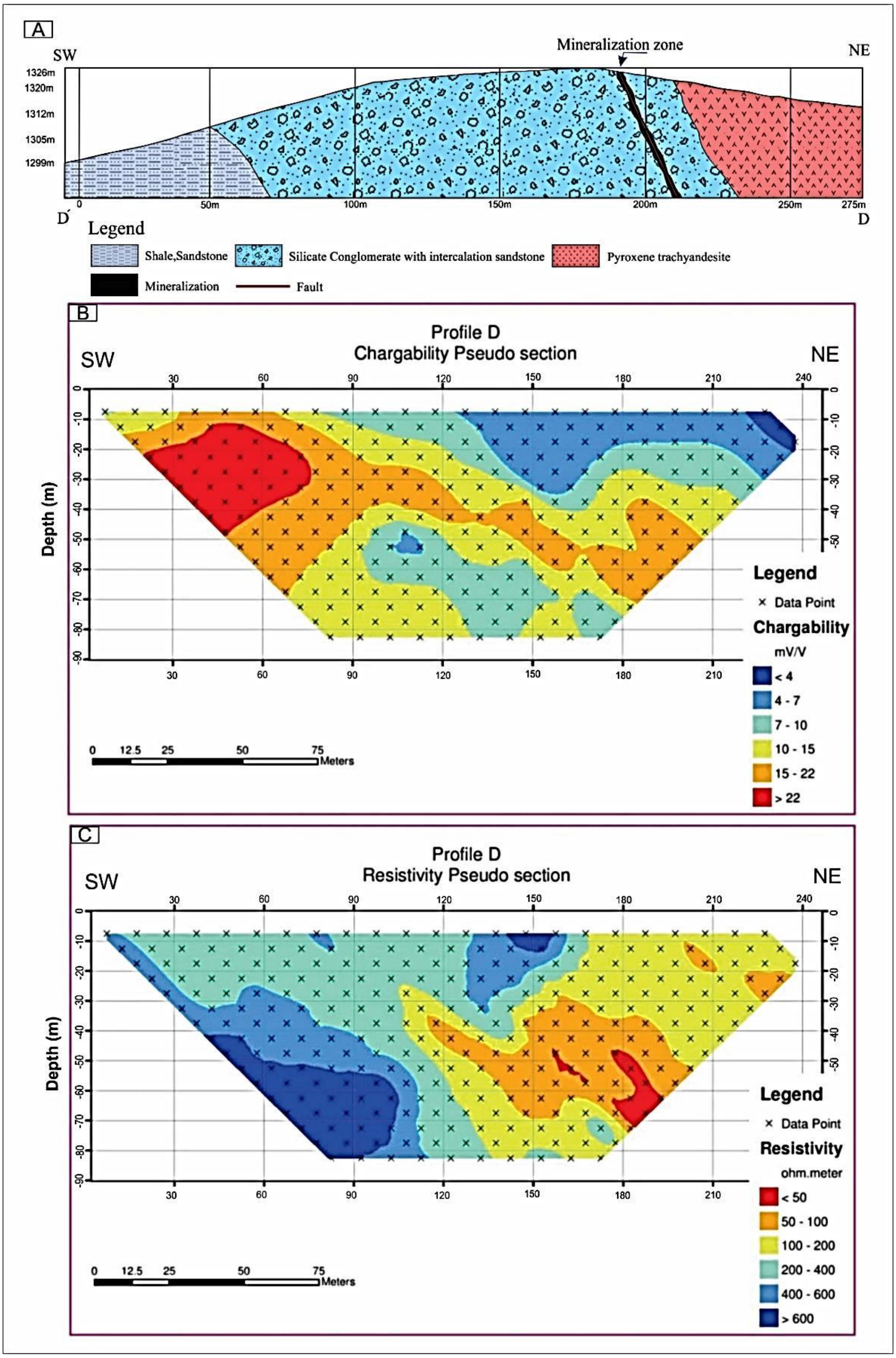

Fig 11. A) The geological profile DD́, B) the pseudo-section of chargeability profile DD́ (Kazem Alilo 2014), C) the pseudo-section of specific electrical resistance of profile DD́ (Kazem Alilo 2014).

7. Results and Discussion

The highest value of chargeability anomalies was observed in IP/RS surveys, which were compatible with the center of the ore-forming vein .The most volume of mineralization was seen in this area. The specific electrical resistance responded well to lithological and alteration changing. Silicification alteration produces high specific electrical resistance. The deeper they were, the lower the specific electrical resistance which may be attributed to a restricted silica content. The highest value of specific electrical resistance in IP/RS profiles are attributable to quartz-rich conglomerates. Specific electrical resistance declines with the emergence of pyroxene trachy-andesite. Specific electrical resistance is inversely related to electrical conductivity, i.e. Locations of highest anomaly of chargeability possess the lowest specific electrical resistance and locations of the lowest anomaly of chargeability possess the highest specific electrical resistance.The medium response by IP suggests a low assay of ore-formation and its restricted expansion. From profiles AA′ in the direction of CC′ in the Zaveh area, the depth and expansion of anomaly decline which suggests that the source of chargeability (probably sulphide mineralization) has been formed in a shallower and less expansive depth along the ore-forming vein from west to east. Based on field studies and microscopic observations, the most significant volume of ore-formation has been formed in the center of the ore-forming vein due to the fact that it best matches with the IP/RS results particularly in AA′ and BB′ profiles and the geochemical analysis. Moreover, a good compatibility was discovered between the value of chargeability, sulphide mineralization and geochemical anomalies based on studies conducted in the Mehrkhash area (Javidi et al. 2015).

Additionally, the 2D and 3D modeling of IP/RS data in a Mongolian copper mine (Zhdanov 2018) have represented a real match between known ore-formations and geophysical surveys. The application of geophysical data and their conflation with ore-formation and geochemical data has also been mentioned in the study implemented in the Mahoor Deposit (Gorabjeiri Puor and Mobasheri 2014). Based on the performed geophysical measurements, Copper mineralization is present in shallow levels in the south and deeper levels in the north of the study area in Central Pontides in Turkey (Ozdemir and Sahinoglu 2018). Zones that have medium chargeability and low specific electrical resistance in the Garmab Copper Deposit (Aadelpour et al. 2016) suggest restricted and disparate ore-formation.

Presence of the highest concentrations of Cu (2.1 gr/T max), Au (56 mlg/T max) and As (>1%) in the center of the vein are compatible with the highest anomalies in chargeability. Even though Au is rare in the area, there is the possibility that the same volume of Au is mainly present in the structure of arsenopyrite. Therefore, based on the IP/RS psedudo-sections, two new points are recommended upstream of the vein for further borings (Table 4).

Table 4: Details of recommend boring operation.

longitude	latitude	Depth(m)	Angle
59°25′44″	35°12′12″	80	90˚
59°25′42″	35°12′12″	90	90˚

The ore-forming event in the Zaveh area is of the vein hydrothermal, Cu, Pb, Zn and As type (Borouziniyat et al. 2019). No signature of intrusive mass has been spotted in the Zaveh area, and what exists is a small outcrop of monzodioritic dykes contiguous to the vein which have been propylitically altered free from any sort of ore-formation. However, it could be deduced from the dyke and granodioritic masses which are scattered out of the study area that magmatism and the semi-deep and deep masses in deep beds that are the source of ore-formation, shall not be excised off the list. There are scattered outcrops of Cu ore-formation around the study area which shall be investigated. It seems that the ore formations have originated from one integrated magmatic source.

5. Conclusion

There is a significant compatibility amongst geophysical, geochemistry and ore-forming data in the exploration of mineral deposits in Zaveh area. According to the field studies and obtained data, the Zaveh deposit is a hydrothermal vein and veinlet of Cu, As, Pb and Zn that are controlled by the fault structure. Geophysical data survey indicates expansive sulphide mineralization in deeper levels. Nonetheless, subterranean data are required to verify this affair. The characteristics of the Zaveh Cu ore-formation suggest another potential of KKBMB. This case and other mining prospects plus the Cu, Au, Fe, Ag, nonmetallic reserves in the northeast of Iran all indicate the importance of further exploration. Applying geophysical methods to further study of the foregoing reserves on one hand and interpretation of data using geochemistry, ore-forming and field studies on the other hand are considered big steps toward more precise exploration of the deposits/reserves, bringing wealth and prosperity to the nation.

Acknowledgement

The authors of the paper are thankful to the Ferdowsi University of Mashhad for providing financial assistance for this research study by grant number 3.41082. We appreciate Moein Sabzehkaran Co. for providing us with reports data. We are also grateful to the friends whose assistance in conducting the field job was critical.

References

Adelpour M Rasa I, Masoudi F and Hosseini M (2016) Determination of Mineralization Zones Using Interpretation of IP and RS Data in The Garmab Copper Deposit (South Khorasan province), *Journal of Economic Geology* 8:129-146 (In Persian).

Aguilef S, Araya Vargas J and Yanez G (2017) Relationship between bulk mineralogy and induced polarisation responses in iron oxide-copper-gold and porphyry copper mineralization, northern Chile, *Exploration Geophysics* 48: 353-362.

Almasi A, Karimpour M H, Hattori K, Francisco Santos J, Ebrahimi Nasrabadi K and Rahimi B (2016) Au-bearing magnetite mineralizaion in Kashmar (alteration, mineralization, geochemistry, geochemistry and fluid inclusions); and Tectono-magmatism of northeast of Iran, *Journal of Economic Geology* 8:61-62 (In Persian).

Barnes H L (1997) Geochemistry of hydrothermal ore deposits, Third edition, New York, John Wiley and Sons 797pp.

Behrouzi A (1987) Geological Map of the Feyz Aabad, Scale 1:100000, Geological Survey of Iran

Borouziniyat B, Malekzadeh Shafaroudi A and Haidarian Shahri M R (2019) Mineralogy, geochemistry, and fluid inclusion studies in Zaveh copper mineralization occurrence, southeast of Torbat-e-Hydarieh, *Journal of Crystallography and Mineralogy* 27:3-18 (In Persian).

Eftekharnejad A, Ala vi Naeini M and Behrouzi A (2004) Geological Map of the Karizno, Scale 1:100000, Geological Survey of Iran.

Ghaemi F and Mossavi Harami R (2006) Geological Map of the Darooneh, Scale 1:100000, Geological Survey of Iran.

Ghaffari M, Rashidnejad-Omran N, Dabiri R, Chen B, Santos JF (2013) Mafic–intermediate plutonic rocks of the Salmas area, northwestern Iran: their source and petrogenesis significance. *International Geology Review* 55(16):2016-29.

Gharib-Gorgani F, Ashja-Ardalan A, Espahbod MR, Sheikhzakariaee SJ, Yazdi A (2017) Petrology of Mg-bearing Meta Ophiolite Complexes of Qaen-Gazik, Eastern Iran, *National Cave Research and Protection Organization* 4(1).

Gorabjeiri Puor A and Mobasheri M (2014) Compiling Data from Geological, Mineralogical and Geophysical (IP/RS)Studies on Mahour Deposit, Northwest of Deh-salm, Lut Block, *Journal of Economic Geology* 7:307-325 (In Persian).

Hoschke T and Sexton M (2005) Geophysical exploration for epithermal gold deposits at Pajingo North Queensland, Australia, *Exploration Geophysics* 36: 401-406.

Javidi moghaddam M, Karimpour M H, Haidarian Shahri M R and Malekzadeh Shafaroudi A (2015) Mineralization, alteration and geochemistry in surface and exploration drill holes and interpretation of IP/RS data in north of Mehr Khash area, Birjand, *Advanced Applied Geology* 16:82-92 (In Persian).

Karimpour M H and Malekzadeh Shafaroudi A (2006) Comparison of the geochemistry of source rocks at Tannurjeh Au-bearing magnetite and Sangan Au-free magnetite deposits, Khorasan Razavi, Iran, Iranian *Journal of Crystallography and Mineralogy* 85:3-26 (In Persian).

Karimpour M H, saadat S and Malekzadeh Shafaroudi A (2006) Geochemistry, petrology and mineralization of Tanurjeh Au-Cu porphyry, *Journal of Science (University of Tehran)* 32:175-185(In Persian).

Kazem Alilo S (2014) Geophysical Operations Report of Zaveh Copper Deposit, Moein Sabzehkaran Co., Organization of Industries and Mines of Khorasan Razavi Province.

Kholghi Khasraghi M H (1990) Geological Map of the Dolat Abad, Scale 1:100000, Geological Survey of Iran.

Kholghi Khasraghi M H (1996) Geological Map of the Torbat-e-Heydarieh, Scale 1:100000, Geological Survey of Iran.

Mahdavi A, Karimpour M H, Haidarian Shahri M R and Malekzadeh Shafaroudi A (2013) Geochemistry and separation of intrusive bodies, their relation with mineralization and interpretation of IP / RS data in the Gazo exploration area, *Advanced Applied Geology* 3:47-60 (In Persian).

Mazhari N, Malekzadeh Shafaroudi A and Ghaderi M (2016) Geochemistry of intrusive rocks, petrology of skarn, and mineralogy and chemistry of ore bodies in the Senjedak-I area, East of Sangan mine, Khaf, NE Iran, *Geosciences* 25:235-246 (In Persian).

Mahdavi M, Dabiri R, Hosseini ES (2015) Magmatic evolution and compositional characteristics of tertiary volcanic rocks associated with the Venarch manganese mineralization, SW Qom, central Iran. *Earth Sciences Research Journal* 19(2):141-145.

Mollai H, Dabiri R, Torshizian HA, Pe-Piper G, Wang W (2022) Cadomian crust of Eastern Iran: evidence from the Tapeh Tagh granitic gneisses. *International Geology Review* 64(10):1372-1392.

Ozdemir A and Sahinoglu A (2018) Geophysical Surveyof Copper Mineralization In Central Pontides, Turkey, *International Journal Of Modern EngineeringResearch* (IJMER) 8:35-49.

Rollinson H (1993) Using geochemical data: evaluation, presentation, interpretation. Longman Scientific and Technical, Essex, UK, 352 pp.

Roshanravan j (2014) End of exploration Report of Zaveh Copper Deposit, Moein Sabzehkaran Co., Organization of Industries and Mines of Khorasan Razavi Province. 10;27(1):3.

Sarem MN, Abedini MV, Dabiri R, Ansari MR (2015) Geochemistry and petrogenesis of basic Paleogene volcanic rocks in Alamut region, Alborz mountain, north of Iran. *Earth Sciences Research Journal* 25(2):237-245.

Shah A, Bedrosian A, P A, Anderson E D, Kelley K D , Lang J R (2009) Geophysical Data Used To Characterize The Regional Setting Of The Pebble Porphyry Deposit in Southwestern Alaska, *Geological Society of America* 41: 493.

Shahrabi M, Hosseini M, Shaabani K (2006) Geological Map of the Bardaskan, Scale 1:100000, Geological Survey of Iran.

Taheri J and Shmaanian Gh (1998) Geological Map of the Kashmar, Scale 1:100000, Geological Survey of Iran.

Tavakoli S, Bauer T E, Rasmussen T M, Weihed P and Elming S A (2016) Deep massive sulphide exploration using 2D and 3D geoelectrical and induced polarization data in Skellefte mining district, northern Sweden, Geophysical Prospecting 64:1602-1619.

Whitney D L, Evans B W (2010) Abbreviations for names of rock-forming minerals, *American Mineralogist* 95:185–187.

Yazdi A, Shahhosseini E, Moharami F (2022) Petrology and tectono-magmatic environment of the volcanic rocks of West Torud–Iran, *Iranian Journal of Earth Sciences* 14 (1): 40-57.

Zhdanov M, Endo M, Cox L, Sunwall D (2018) Effective-Medium Inversion of Induced Polarization Data for Mineral Exploration and Mineral Discrimination: Case Study for the Copper Deposit in Mongolia, *Minerals* 8:68.